Journal of the Earth & Space Physics. Vol. 38, No. 2, 2012, P. 1-15

Detailed crustal discontinuities, seismotectonic and seismicity parameters of the east-middle Alborz, Iran, flower structure of subsurface fault geometry

Nemati, M.[1*], Talebian, M.[2], Sadidkhouy, A.[3], Mirzaei, N.[4] and Gheitanchi, M. R.[5]

[1] *Assistant Professor, University of Kerman, Science faculty, Geology department, Kerman, Iran and Assistant Professor, Geological Survey of Iran, Tehran, Iran*
[2] *Assistant Professor, Geological Survey of Iran, Tehran, Iran*
[3] *Assistant Professor, Institute of Geophysics, University of Tehran, Iran*
[4] *Associate Professor, Institute of Geophysics, University of Tehran, Iran*
[5] *Professor, Institute of Geophysics, University of Tehran, Iran*

(Received: 17 Jan 2010, Accepted: 31 Jan 2012)

Abstract

The investigation of this paper focuses on eastern part of Shahroud fault system in middle-east Alborz. This fault system is an important part in the seismotectonic map of the area. We used two local temporary dense seismological networks data installed around the fault system for several months during 2007 and 2008 and simultaneously micro-earthquakes data recorded by the permanent seismological network of the Geophysics Institute of University of Tehran were used. The seismicity of both networks has overlapping with the surface outcrops and the depth of Shahroud fault system faults, mainly Astaneh fault. Processing the data provided us a P wave velocity range within the east Alborz which resulted discontinuities like seismogenic zone thickness, 24 km. An initial estimation of Moho depth located at 34 km, near vertical and north dipping seismicity dips corresponding with the Astaneh and North Semnan faults respectively were the other results. Faults dipping and seismogenic zone thickness do not support the flower structure hypothesis at the east Alborz in spite of some author's idea. A few focal mechanisms indicated left-lateral motion and confirm high angle of the faults planes. The crustal movement directions resulted from P and T vectors show well correspondence with the GPS measured direction in the area. The b-value which could be considered as inverse short term background seismicity intense, was determined about 0.9.

Key words: Shahroud fault system, Micro earthquake, Crustal velocity, Flower structure and East Alborz

ناپیوستگی‌های پوسته، لرزه‌زمین‌ساخت و ویژگی‌های لرزه‌ای البرز خاوری- میانی، ایران، بررسی ساختار رزگون برای هندسه ژرفی گسل‌ها

مجید نعمتی[۱]، مرتضی طالبیان[۲]، احمد سدیدخوی[۳]، نوربخش میرزائی[۴] و محمدرضا قیطانچی[۵]

[۱] *استادیار، دانشگاه باهنر کرمان، دانشکده علوم، بخش زمین‌شناسی، کرمان، ایران و استادیار، سازمان زمین‌شناسی و اکتشافات معدنی کشور، تهران، ایران*
[۲] *استادیار، سازمان زمین‌شناسی و اکتشافات معدنی کشور، تهران، ایران*
[۳] *استادیار، موسسه ژئوفیزیک دانشگاه تهران، ایران*
[۴] *دانشیار، موسسه ژئوفیزیک دانشگاه تهران، ایران*
[۵] *استاد، موسسه ژئوفیزیک دانشگاه تهران، ایران*

(دریافت: ۸۸/۱۰/۲۷ ، پذیرش نهایی: ۹۰/۱۱/۱۱)

*Corresponding author: Tel: 0341-3222035 Fax: 0341-3222035 E-mail: majidnemati1975@yahoo.com

چکیده

رشته‌کوه البرز که به دنبال برخورد پهنه‌های عربی و اوراسیا در تریاس پسین شکل گرفته و آهنگ کنونی این برخورد ۲۱ میلی‌متر در سال است، گستره‌ای چین‌خورده، گسل‌خورده و یکی از گستره‌های کوتاه‌شدگی پوسته زمین در ایران است. ایالت لرزه‌زمین‌ساختی البرز از شمال به گسل خزر، از جنوب به گسل‌های مشا، طالقان، شمال قزوین، شمال تهران، شمال سمنان وآستانه، از غرب به کوه‌های طالش و از شرق به ایالت لرزه‌زمین‌ساختی کپه‌داغ کران دارد. جابه‌جایی البرز شرقی به دو جابه‌جایی راندگی گسل خزر و جابه‌جایی راستالغز چپ‌گرد سامانه گسلی شاهرود با راستای شمال شرقی – جنوب غربی افراز (Partitioning) می شود. گسل‌های سامانه گسلی شاهرود و سازوکار زمین‌شناسی همگی آنها در روی زمین شناخته شده است، اگرچه هندسه آنها در ژرفا شناخته شده نیست. این گستره لرزه‌خیز پیش‌تر مورد بررسی‌های لرزه‌خیزی قرار نگرفته است.

به‌جز زمین‌لرزه ۲۰-۰۱-۱۹۹۰ با سازوکار راستالغز چپ‌گرد (هاروارد، ۲۰۱۱) و وابسته به گسل فیروزکوه، زمین‌لرزه دیگری با سازوکار معلوم در گستره یادشده وجود ندارد. بنا به دلایل بالا راه اندازی شبکه های محلی برای بررسی ساختار سرعتی پوسته در البرز شرقی و پراکندگی خُردلرزه‌ها برای بررسی جنبایی گسل‌ها در این گستره، گریز ناپذیر بود. پاره شرقی سامانه گسلی شاهرود در گستره البرز خاوری در این نوشتار پژوهشی بررسی شده است. این سامانه گسلی بخش مهمی در نقشه لرزه‌زمین‌ساختی این گستره به شمار می‌رود. زمین‌لرزه تاریخی سال ۸۵۶ کومس را که بزرگ‌ترین زمین‌لرزه درون قاره‌ای ایران است می‌توان به سامانه گسلی شاهرود وابسته دانست. همچنین زمین‌لرزه تاریخی سال ۱۳۰۱ با بزرگی ۶/۷ و زمین‌لرزه‌های دستگاهی ۱۸۹۰ و ۱۹۳۵ به شماره با بزرگی‌های ۷/۲ و ۵/۸ در نزدیکی گستره بررسی شده روی داده‌اند که می‌توان آنها را نیز به سامانه گسلی شاهرود وابسته دانست.

در این بررسی دو شبکه لرزه‌نگاری محلی (سازمان زمین‌شناسی و اکتشافات معدنی کشور) با ایستگاه‌های نزدیک به هم در مدت زمان ۹ ماه پیرامون این سامانه گسلی راه‌اندازی شدند و داده برداشت کردند. همچنین هم‌زمان از خُردلرزه‌های برداشت شده با شبکه‌های لرزه‌نگاری موسسه ژئوفیزیک نیز بهره جستیم. پراکندگی زمین‌لرزه‌هایی که به تنهایی با ایستگاه‌های شبکه‌های لرزه‌نگاری موسسه ژئوفیزیک برداشت شده‌اند، به دلیل فاصله زیاد میان‌ایستگاهی، هم‌خوانی خوبی با هندسه سطحی و ژرفی گسل‌ها ندارند. پس از ویرایش و پردازش داده‌ها، با به‌کارگیری روش واداتی (۱۹۳۳) وابستگی V_P/V_S با ضریب همبستگی ۰/۹۸ مقدار ۱/۷۱، و بازه ۴ لایه‌ای سرعت پرتو لرزه‌ایP میان ۵/۴ تا ۸/۰ کیلومتر بر ثانیه از سطح تا گوشته بالایی نیز به‌دست آمد. رومرکز زمین‌لرزه‌های هر دو شبکه محلی با رخنمون سامانه گسلی نامبرده به‌ویژه مهم‌ترین پاره گسلی آن (گسل آستانه) هم‌پوشانی داشتند.

با سنجش آماری دو دسته زمین‌لرزه برداشت شده با شبکه‌های محلی و شبکه‌های لرزه‌نگاری موسسه ژئوفیزیک، به سادگی می‌توان کمتر بودن خطاها را در زمین‌لرزه‌های شبکه محلی دریافت. در این بررسی ستبرای نهشته‌های رویی نزدیک به ۴ کیلومتر، مرز لایه بلورین رویی در ۱۳ کیلومتری، پهنای لایه لرزه زا ۲۴ کیلومتر و یک برآورد اولیه از ژرفای موهو ۳۴ کیلومتر به‌دست آمد. ژرفای ناپیوستگی‌های موهو و لایه لرزه‌زا با به‌کارگیری پردازش زمان سیر پرتوهای شکسته مرزی گذرنده از زیر ناپیوستگی‌ها به‌دست آمده‌اند.

همچنین برای ژرفای لایه لرزه‌زا از پراکندگی ژرفی زمین‌لرزه ها استفاده شده است. دو شیب تند و یک شیب رو به شمال به شماره، برای گسل‌های آستانه، چاشم و شمال سمنان پیشنهاد شد. ژرفای بیشتر زمین‌لرزه‌ها از ۴ تا ۱۴ کیلومتری است. این پراکندگی نشان می‌دهد که بیشتر زمین‌لرزه ها در درون لایه بلورین رویی رخ داده‌اند. با اینکه شیب همه گسل‌های جنوبی گستره (مانند گسل‌های گرمسار و شمال سمنان) رو به شمال و شیب همه گسل‌های شمالی گستره (مانند گسل‌های خزر و شمال البرز) رو به جنوب هستند، به دلیل ستبرای کم لایه لرزه‌زا نمی‌توان بر وجود ساختار رزگون (گلی) در البرز شرقی پافشاری کرد. دلیلی نیز برای کمتر شدن شیب آنها در ژرفا در دست نداریم تا در لایه لرزه‌زا به هم برسند.

راستای بردارهای تنش لرزه‌ای، که از سازوکار خُردلرزه‌ها برگرفته شده‌اند، با راستاهای جابه‌جایی اندازه‌گیری شده با GPS هم‌خوانی دارند. این بردارها نیروی کششی را در راستای شمال غربی– جنوب شرقی و راستای فشار را عمود بر آن نشان می‌دهند. از پارامترهای لرزه‌خیزی، b-Value که وابسته به عکس توان لرزه‌ای گستره و متناسب با نسبت احتمال رخداد زمین‌لرزه‌های کوچک به بزرگ است، نزدیک به ۰/۹ به‌دست آمد. ازآنجاکه این پارامتر وابسته به بزرگی نیست پس می‌توان آن را برای لرزه‌خیزی زمینه نیز به‌دست آورد.

واژه‌های کلیدی: سامانه گسلی شاهرود، خُردلرزه، الگوی سرعتی پوسته، ساختار رزگون و البرز شرقی

1 Introduction

The east Alborz is one of active seismological regions in the Alpine-Himalaya zone. This region has experienced important earthquakes. Based on geological maps of the area (Geological Survey of Iran (GSI)), Shahroud fault system which is recognized by Astaneh, Firuzkuh and two medium thrust faults, Bashm and Chashm, is a significant part of the east Alborz. The Shahroud fault system undertakes left lateral part of motion of the east Alborz. About two million people live around the fault system in Semnan, Shahroud and the other small cities (negotiation with the Governmental authorities). All of the faults in Shahroud fault system were mapped and their surface mechanisms were specified; but their related geometry at depth and seismicity were not characterized. We determined characteristics of the faults especially the Astaneh fault in surface and depth during 9 months the seismic energy released and. We analyzed the waveform of the small earthquakes recorded around Shahroud fault system, using two local networks (GSI) installed for 9 months. Also two years data of network of the Geophysics Institute of University of Tehran (IGUT) in the east Alborz were used. Indeed the studied area was selected determining crustal velocity discontinuities and to investigate seismic activity of the faults especially Astaneh fault. Due to lack of seismological data for recognition sub-surface tectonic of the faults, there was no comparison to the measured characteristics in the surface during paleoseismological investigation (GSI) in the research area.

2 Tectonic setting

The Alborz Mountains formed following Arabia-Eurasia collision dated Late Triassic (Sengor et al., 1988), see Fig. 1. Alborz range has north-south shortening and is impressed from the south by central Iranian block (Vernant et al., 2004a). The range has been made by sedimentary and Paleogenic thick sequences (Stöcklin, 1974; Berberian and King, 1981). There are many important evidences for uplifting (river and coastal marine terraces) of the mountains (Berberian, 1983) and over-thrusting the range on the South Caspian Basin (SCB) (Tatar et al., 2007) which comes from it's seismically activity. The maximum altitude is a Quaternary volcano pick of Damavand (Jackson et al., 2002) which increases the depth of Moho (~67.5 km) just under the pick (Sodoudi et al., 2009). Regarding to the earthquakes dominant mechanism (Harvard) of Alborz, the faults move strike slip left laterally paralleled to the range. The east Alborz has intense relationship to the SCB, which is one of important regions seismotectonically. The faults left lateral motion in the east Alborz has coherency with the northwestward motion of the SCB (Hollingsworth et al., 2008) and with the clockwise rotation of the SCB (Ritz et al., 2006). Regarding to globally gravity investigations, except Damavand, there is not root and increase in the depth of the Moho in the Alborz (Dehghani and Makris, 1984). The Receiver Functions (RFs) study of Sodoudi et al., (2009) indicates missing crustal root of the central Alborz. They concluded sub-lithospheric mantle could be responsible for the elevation of the mountain.

The Alborz has been bounded by important faults and the areas, like Astaneh and Firuzkuh faults (Shahroud fault system) from the southeast and Kopet Dagh seismological province from east. According to geological maps (GSI), the faults are so clearer in the east of the range than the west. The deformation of the east Alborz is partitioned to Khazar thrust fault and left lateral motion of Shahroud fault system (Jackson et al., 2002). All of the mentioned faults participate to convergence perpendicular to the range (Allen et al., 2003). Most of the faults in the studied area are high angle (Khazar fault is south dipping) and have left lateral strike slip motion, based on microearthquake distribution recorded by the IGUT network (this paper), morphotectonic studies (Jackson et al., 2002) and paleoseismological attestation (Ritz et al., 2006). There is an unmapped fault as the

boundary of mountains and flat in the south of studied area (hereafter called North Semnan or N. Semnan fault).

Astaneh fault, the case study of the local networks has about 100 km length, based on 1:250000 geological map of Semnan (Samadian et al., 1975) and Sari (Vahdati and Saidi, 1991). This fault has made a left lateral pull-apart basin near 53.6°E. A left lateral alluvial fan deposits displacement formed near 54°E (Hollingsworth et al., 2008). The fault had initially introduced as thrust with southward dipping (Berberian et al., 1996) and now is considered as left lateral strike slip fault (Jackson, et al., 2002; Ritz et al., 2006)). However, a NNW-SSE geological section (Samadian et al., 1975 and Vahdati and Saidi, 1991) indicates different; Astaneh fault has acted as a thrust on a core of an anticline, has repeated the Mesozoic limestone and shale formations and also is partitioned to two branches near 53.5°E.

Astaneh fault is connected to Firuzkuh fault via above-mentioned south dipping and north dipping thrust segments, Chashm and Bashm faults respectively (west segments of the Astaneh fault (Fig. 1). These segments have acted, as a graben, on the core of the mentioned anticline at the studied area (Samadian et al., 1975).

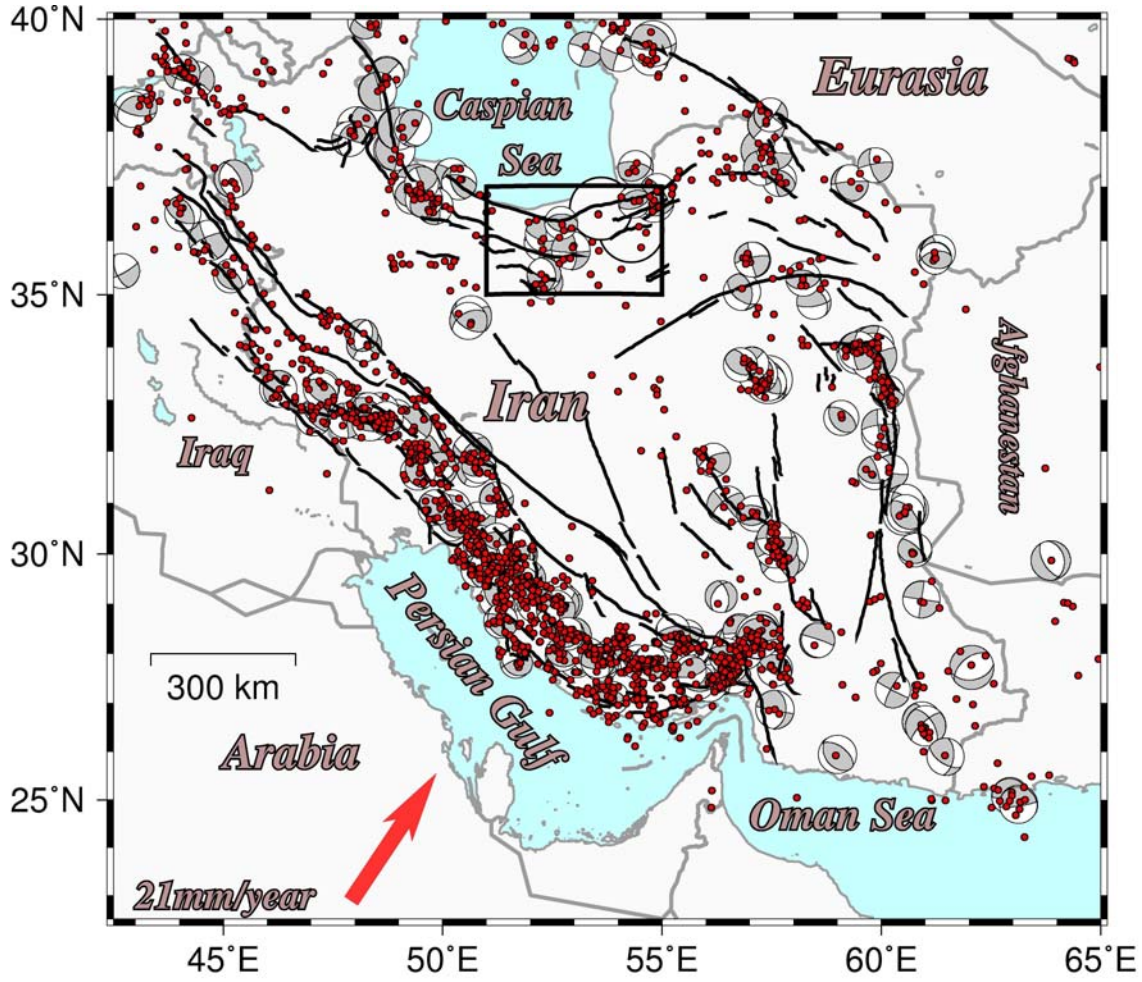

Figure1. A view shows crustal shortening in the Alborz and Zagros area following Arabia-Eurasia encounter with the rate of 21 mm/year (red arrow) (Vernant et al., 2004b). The rectangle shows studied area, open circles indicate Qumes and 1935 earthquakes and red circles specify relocated earthquakes (Engdahl et al., 1998).

Table1. The historical and instrumental (*) earthquakes in the central and east Alborz (Ambraseys and Melville, 1982).

Date	Longitude (E°)	Latitude (N°)	Magnitude	Date	Longitude (E°)	Latitude (N°)	Magnitude
400 B.C.	51.8	35.5	7.6	1830-03-27	52.5	35.7	7.1
743	52.2	35.3	7.2	1830-04-06	52.6	35.9	-
856-12-22	54.3	36.2	7.9	1852-03 25	54.3	35.9	-
859	54.3	36.2	-	1868-07-01	52.5	34.9	6.4
1301	53.2	36.1	6.7	1890-06-11	54.6	36.6	7.2
1665	52.1	35.7	6.5	1890-01-15	54.7	36.6	-
1805	52.4	36.2	-	1927-06 22	53.64	34.72	6.3
1808	52.4	36.2	-	1930-09 02*	52.08	35.86	5.2
1809	52.5	36.3	6.5	1933-03-05*	53.21	35.91	5.8
1815	52.2	35.9	-	1935-04-11*	53.61	36.59	6.8
1825	52.6	36.1	6.7	1957-06-02*	52.70	36.14	6.8

3 Historical seismicity

Many earthquakes occurred in the central and east Alborz. Table 1 shows historical and instrumental earthquakes occurred in the research area and around. The historical earthquake of 856 of Qumes and instrumental earthquake of 1935 with estimative epicenter could be related to the Shahroud fault system. The destructive Qumes earthquake killed about 200,000 people in Damghan and environs (Ambraseys and Melville, 1982).

Figure 1 shows a view of studied area in the regional tectonic regime and the location of major faults (GSI). About the regional seismicity we could say master event technique helps increase the accuracy of the teleseismic earthquake location (Engdahl et al., 1998), but there are only a few events have been relocated in the studied area. There is not any earthquake in survey area with known mechanism except the earthquake of 1990 with left lateral strike slip mechanism, shown at the middle of the rectangle in Fig. 1, related to Firuzkuh fault (Harvard). Therefore, any interpretation based on these data is not so reasonable. We have done scrutiny in the area because of lack of seismological data. This paper has determined crustal structure and micro earthquake locations to explain kinematics and seismic activity of the faults.

4 Acquisition and processing the data

We used 10 temporary among 10 permanent stations in each network to investigate the area (Fig. 2). We installed two dense local networks (2007-2008 and 2008) each consists of 10 medium band CMG-3ESP (Güralp LTD) instruments with cut-off period of 60 s. The permanent short period instruments are SS1 and have nanometeric system. The local networks instruments belong to GSI and nanometeric system instruments belong to telemetry seismological network of IGUT. The instruments of the IGUT are short period of three components. The duration of the 2007-2008 network was from October 2007 to April 2008 and the duration of the 2008 network was from June to December of 2008. Fig. 2 shows the permanent and temporary stations on the map.

The instruments recorded the waveform data in a continuous mode, at 100 (Hz) sampling rate. The temporary stations were

visited every week for maintenance, checking their power supplies and internal time against the time of the external GPS of the instruments. The P_g and S_g phases of the events were read. The appropriate horizontal amplitudes were picked to calculate M_L with Wood-Anderson (WA) method that removes any response of the instruments and supposes them as Wood-Anderson displace-meters.

For obtaining the velocity model, we estimated the V_P to V_S ratio from dips of six Wadati (Wadati, 1933) diagrams of t_S-t_P versus t_P, using local networks and IGUT network data. The least square method was used adjusting the line in the diagrams. We used 6 exact recorded local earthquakes and concluded average $V_P/V_S = 1.71$ (Fig. 3).

We adopted initial shallow velocity model from Nemati et al. (2010) shown in table 2. We optimized our previous velocity model using another selected events arrival times by 1D inversion program (Kissling, 1988). For computing, 68 events recorded with minimum 8 phases, maximum azimuth gap of 180°, RMS less than 0.2 s and both horizontal and vertical uncertainties less than 2.0 km were used. First randomly many models should be tested. After testing a few thousands multilayer models, in order to converge of the inversion to a unique velocity model, 50 random models were tested. Each model was stacked of 15 layers with 2.0 km thickness from the surface to 30 km depth, with maximum 0.5 km/s velocity change for each layer from the uniform starting velocity of 6.0 km/s. Those thin layers and little velocity changes allowed us to determine the approximate depths and velocities of the real layers. We suggested a three-layer model with three velocity contrasts located at 4, 10 and 14 km depth over a half space. After merging the layers with the similar velocities, the starting model was repeated with the mentioned contrasts and the same velocity of the first step (Fig. 4). Table 2 shows the initial and computed velocity model. Because majority of the events was located shallower than 20 km, we could not suggest any layer beneath this depth using the inversion because the inversion is possible only for the shallow crust above the events.

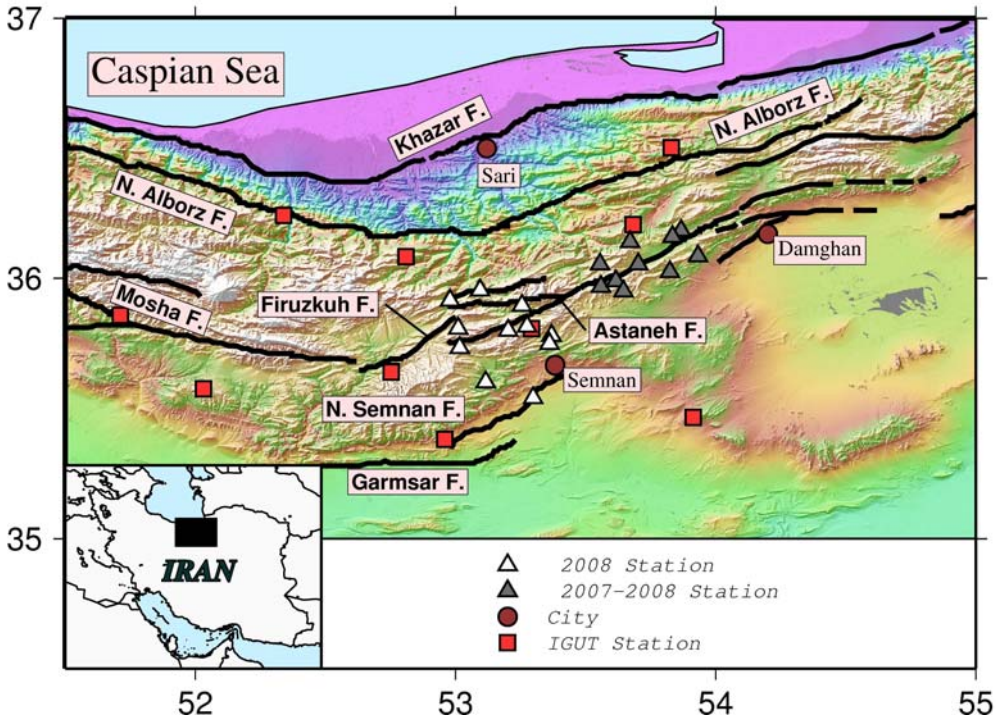

Figure2. Survey area and the permanent and temporary stations used to investigate the middle and east Alborz and the location of the faults (GSI).

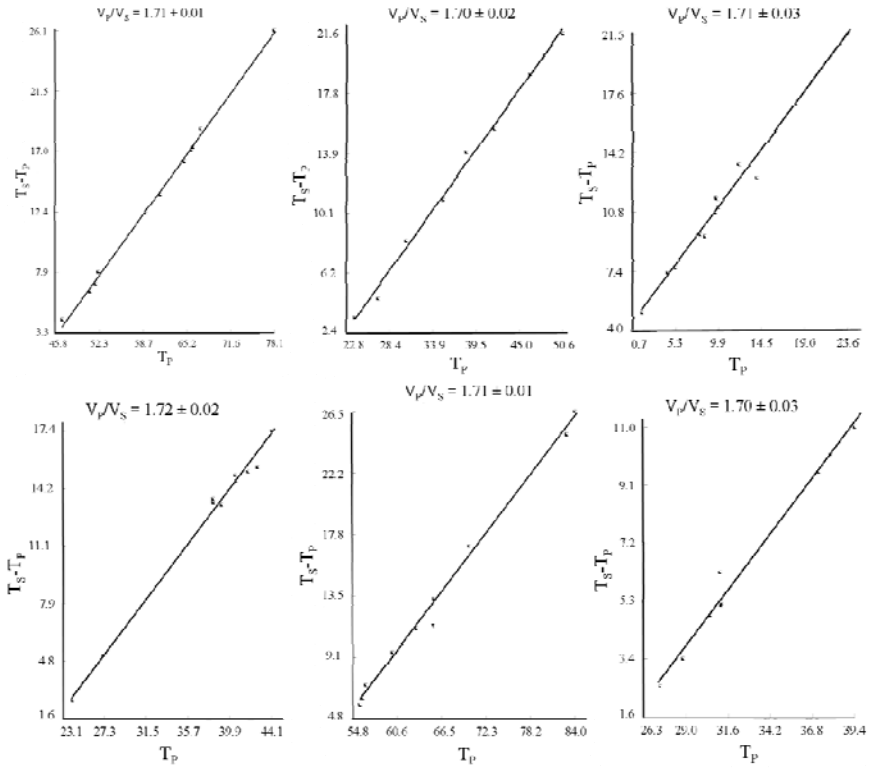

Figure3. Diagrams show the plots of the t_S-t_P versus t_P using local and IGUT networks data. We used selected earthquakes from recorded data with minimum 6 phases, RMS less than 0.3 s, both horizontal and vertical errors less than 3 km, azimuth gap less than 180° computing the V_P/V_S. Each dot in the diagrams shows one station and the best fitted line was drawn by least square method.

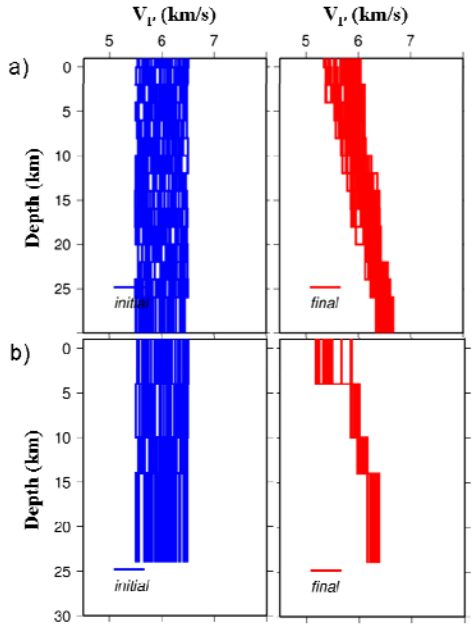

Figure4. Computed 1-D velocity model using travel times of the locally recorded events with inversion method, (a) A multilayer (thickness of 2-km) model of homogeneous velocity that randomly modified was tested, (b) Simplification of the result of the first inversion to refine the final velocity model.

Analyzing of arrival times, P and S phases, of locally recorded micro earthquakes (Ashtari et al., 2005) shows 34 km for depth of the Moho discontinuity and 8.0 km/s for velocity of the upper mantle in south of Alborz up to longitude of 52.5°E without presence of any other estimation. Although Asudeh (1982) processing is an old and unique estimation of the Moho depth at the eastern Alborz. According to 2D migrated RFs analysis with IGUT network stations in a W-E profile at the latitude of 35.3°N in the central Alborz, the average depth of the Moho obtained 44-46 km. Regarding to this study there is increase in the Moho depth, only under Damavand station (Sodoudi et al., 2009). Also Abbassi et al. (2010) and Rajaee et al. (2010) using jointly inverted Receiver Functions method estimated average 52 km for this depth at 50 km west of studied area. We calculated the depth of the seismogenic layer and the velocity of the lower crystalline crust were obtained 24 km and 7.9 km/s using 424 phases with an RMS less than 0.5 s for the local events which recorded nearer than 350 km (Fig. 5a). Also 8.03 ± 0.07 km/s for P_n as the velocity of upper mantle and 34 km for depth of the Moho (Fig. 5b) obtained using travel times of 458 phases of the IGUT network distant events recorded with minimum 6 phases, with RMS less than 0.5 s and the epicentral distance less than 350 km. The refractive method is efficient only for level discontinuities. Figures 4 and 5 show discontinuities computed using inversion and refractive ray path methods of distant earthquakes respectively.

5 The seismicity

We relocated the earthquakes of the IGUT network, using Hypo71 program (Lee and Lahr, 1972), from January 2006 to February 2009. We selected 602 events from totally 1443 events recorded by the network during this period. Because of having a view of the seismicity of the central and east Alborz, we did not select the epicenters for maximum azimuth gap. The temporary networks during 2007 and 2008 recorded 1972 earthquakes which we selected 291 events. There were only a few explosions in the area because time distribution of the data did not show more explosions, which usually occur in specific times during the day. Quarries in around mines were responsible for the explosions that were removed from the data. Fig. 6 shows distribution pattern of the events and Fig. 7 shows the statistics of the local networks and the IGUT network earthquakes. According to the distribution pattern of the earthquakes, the seismic activity has been concentrated near Astaneh and North Semnan faults and less associated with Firuzkuh, Mosha, Garmsar, North Alborz and Khazar faults. The seismicity shows the north branch of the Astaneh fault (acted as a thrust fault in the geological map of Semnan) that joints the Astaneh and Firuzkuh faults, is more active than the south one.

Table2. Initial and computed velocity structure imputing travel times of the locally recorded events into inversion and refraction methods.

Initial		Final	
Velocity (km/s)	**Depth (km)**	**Velocity (km/s)**	**Depth (km)**
		5.5	**0.0**
5.40	**0.0**	**6.0**	**4.0**
6.00	**4.0**	**6.2**	**10.0**
6.30	**12.0**	**6.4**	**14.0**
		7.9	**24.0**
		8.0	**33.5**

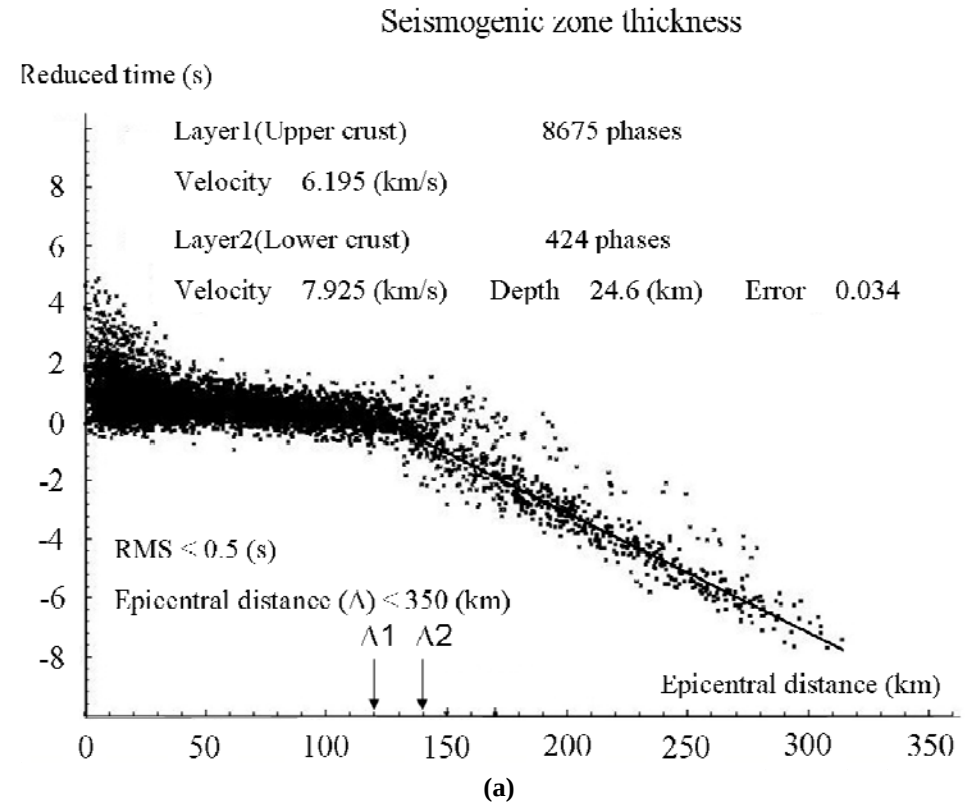

(a)

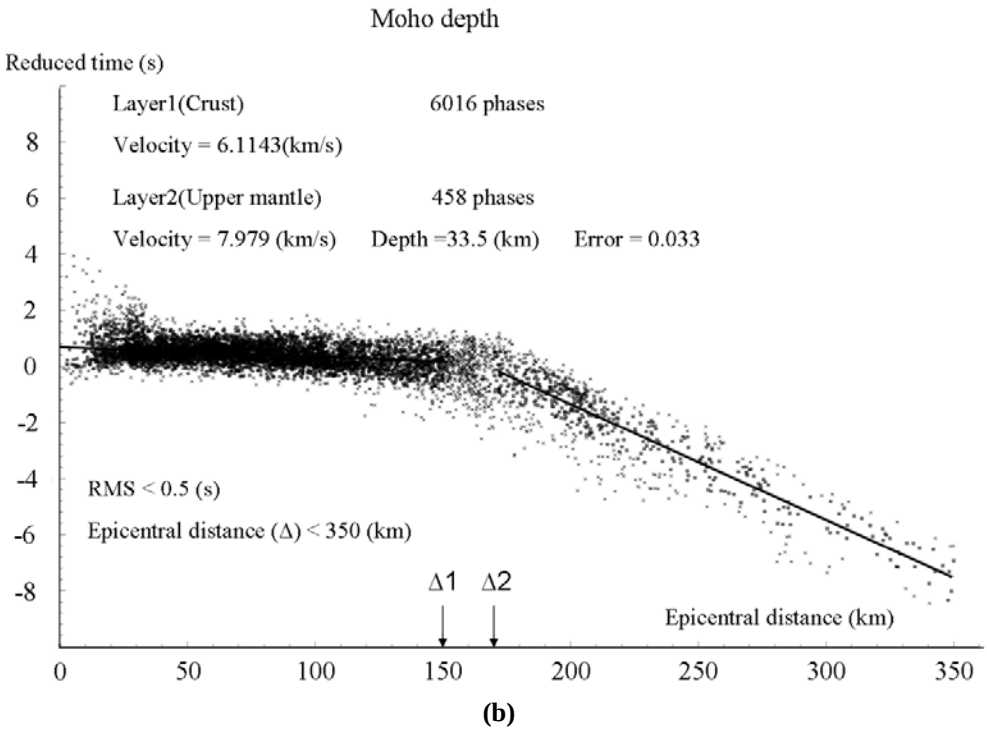

(b)

Figure5. (a) Estimation of the depth of the seismogenic layer and velocity of lower crystalline crust using travel times of distant earthquakes recorded with the local networks. (b) Initial estimation of the depth of the Moho and velocity of the upper mantle using travel times of distant earthquakes recorded with the IGUT stations. The depth of the layers was reasonably well constrained by the intercept between Δ_1 and Δ_2.

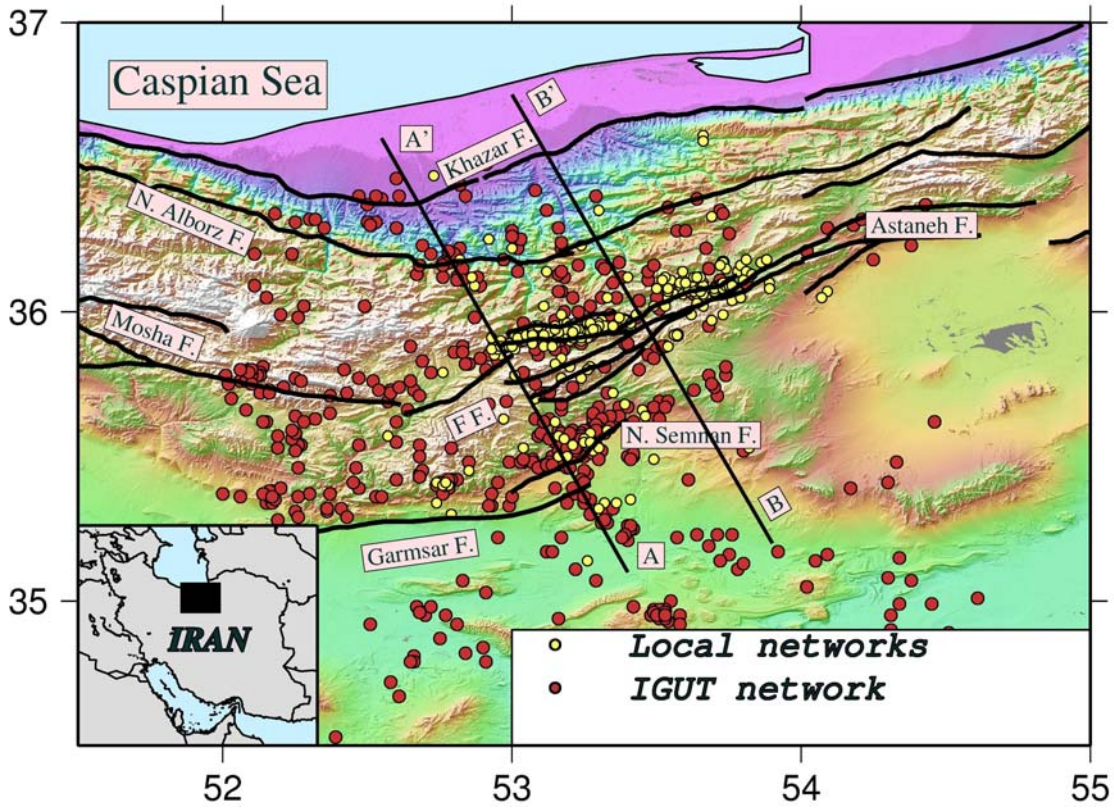

Figure6. Seismicity of the IGUT network recorded with more than 6 phases, with RMS less than 0.4 s, uncertainties in both location and depth less than 5.0 km (red circles) and seismicity of the selected earthquakes of the local networks recorded with more than 7 phases, an RMS less than 0.3 s, azimuth gap less than 270°, uncertainties in both location and depth less than 3.0 km (yellow circles). The data relocated with Hypo71 program (Lee and Lahr, 1972). FF indicates to Firouzkuh fault.

The majority of the local networks earthquakes were concentrated near Astaneh fault. The seismicity in Fig. 6 shows that the activity of the fault has been concentrated on north partitioned segment. Thickness of 4 km is suggested for the sedimentary cover deduced by velocity structure. Depth distribution of the earthquakes has been shown in Fig. 8a and in diagram of Fig. 8b. The red columns of the histogram (local networks data) show a sharp pick in 8 km within 2 and 14 km main distribution range. The range is considered as the seismogene upper crystalline crust at the east Alborz.

To illustration the geometry of the faults especially Astaneh fault at depth, we plot 2 cross-sections perpendicular to the Alborz tectonic structure (A-A' and B-B') in the area (Fig. 8). For better display of the seismicity dips at the depth, widths of cross-sections were selected 20 km. The seismicity dips related to the Astaneh fault are high angle and the seismicity dip related to the N. Semnan fault is steep north-dipping. The mentioned faults dipping could not suggest flower structure as the sub-surface geometry of the faults. Because of having no well located earthquakes deeper than 24 km and having a discontinuity in 24.6 km (Fig. 5a), the range of 24 km has considered as the seismogenic zone thickness in the area. As shown in Fig. 8b there are obvious overlap between the event number and the velocity jumps in specific depths especially for 14 and 24 km. Figure 9 shows the map of the focal mechanisms which confirms the left lateral strike slip motion of the Astaneh fault. The focal characteristics have been shown in appendix 1.

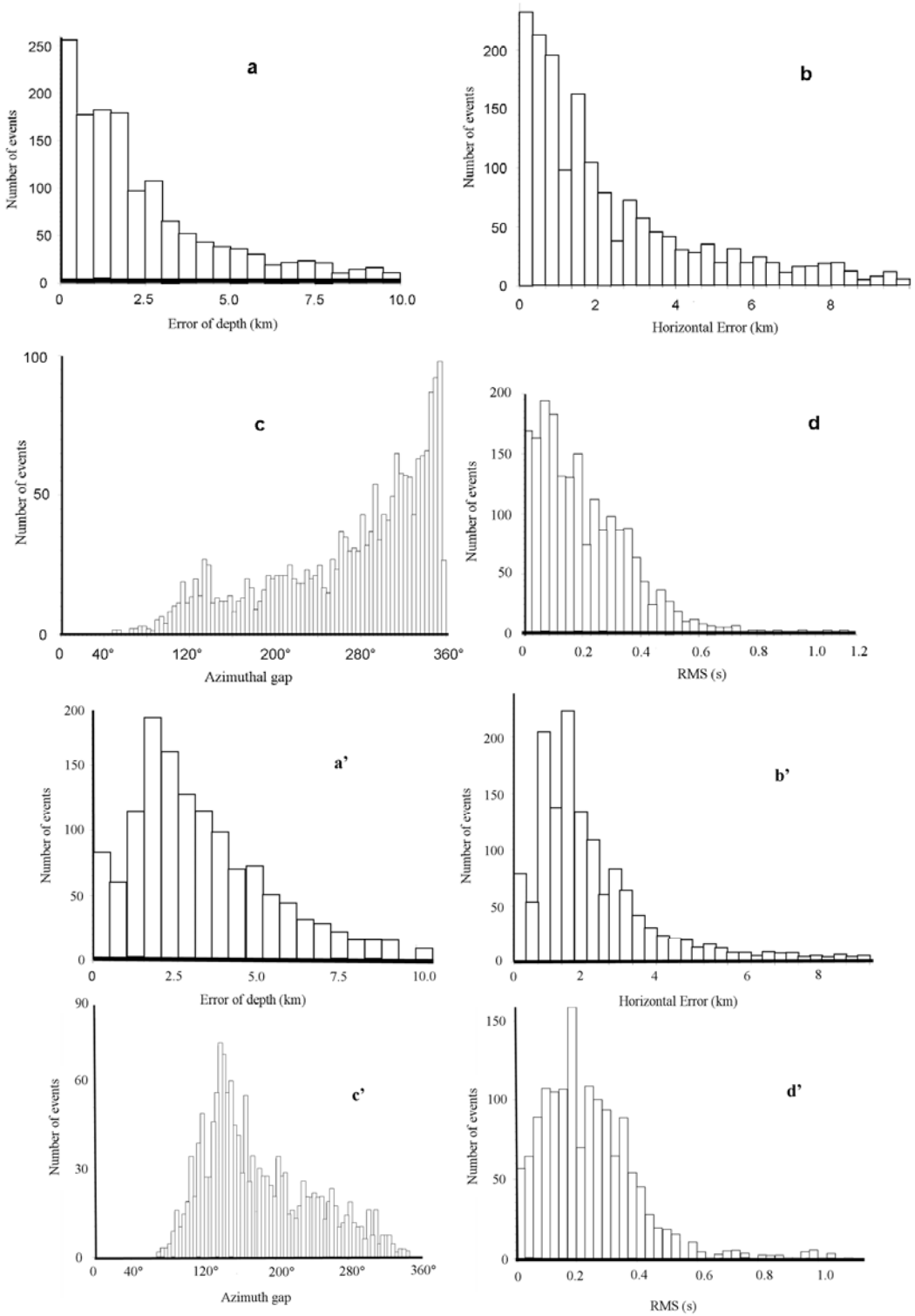

Figure7. The diagrams a, b, c and d show the statistics of the local networks earthquakes. The diagrams a and b show that the location (horizontal and vertical) errors of about 60% of the earthquakes are less than 3 km, diagram d shows that RMS of about 60% of the earthquakes is less than 0.3 s and finally diagram c shows that only about 40% of them are inside the networks. The diagrams a', b', c' and d' show the statistics of the IGUT network earthquakes.

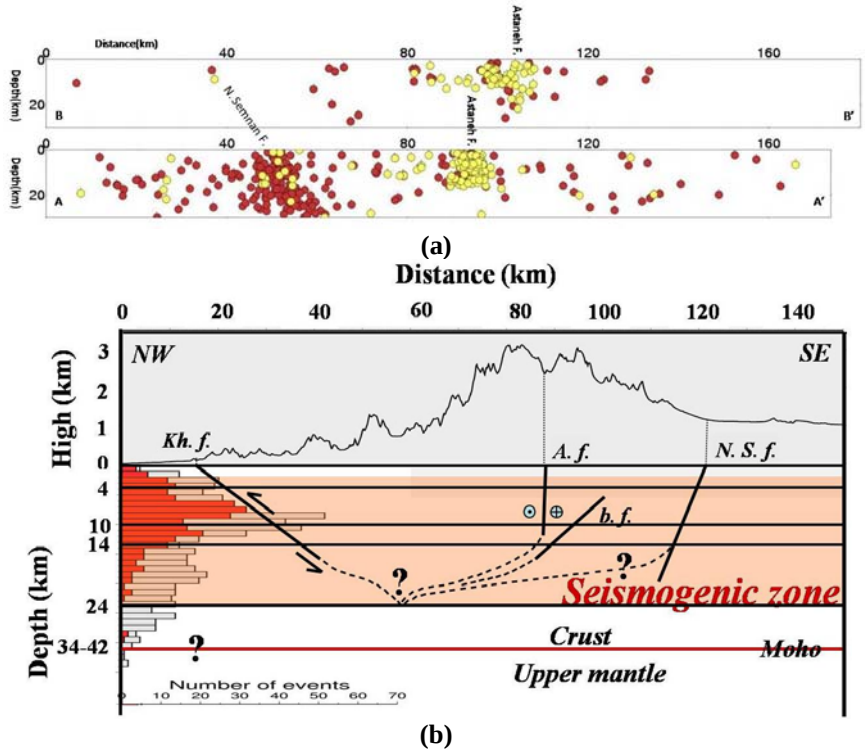

Figure8. (a) Cross-sections (A-A' and B-B') show the depth distribution of the earthquakes of Fig. 6. The width of cross-sections are 20 km. b) A schematic cross-section parallel to A-A' shows impossibility of flower structure of the faults in the east Alborz. The length and dips of the Astaneh and N. Semnan faults drawn using depth distribution of the earthquakes in A-A' and B-B' and of the Khazar fault (34°dip) was taken from Tatar et al. (2007). The Kh. f. shows Khazar fault, A. f. specifies Astaneh fault. (b) f. indicates blind fault and N. S. f. characterizes North Semnan fault. The topography does not have the same vertical and horizontal scales. The red columns of the histogram show the local networks events and the white columns show IGUT events. The lower crust is not scaled.

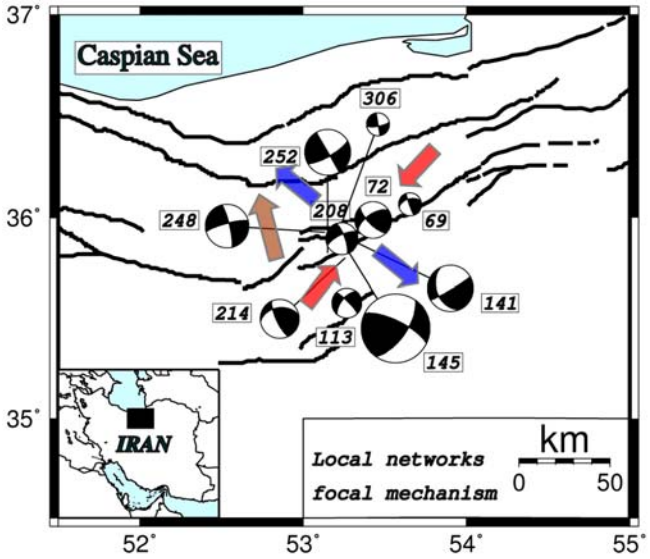

Figure9. Map of the focal mechanisms and the consequent compression P and tension T axes show general shortening in direction of NE-SW (red arrows), extension in direction of NW-SE (blue arrows) and Firuzkuh GPS station measured direction (brown arrow) (Vernant et al., 2004a and b).

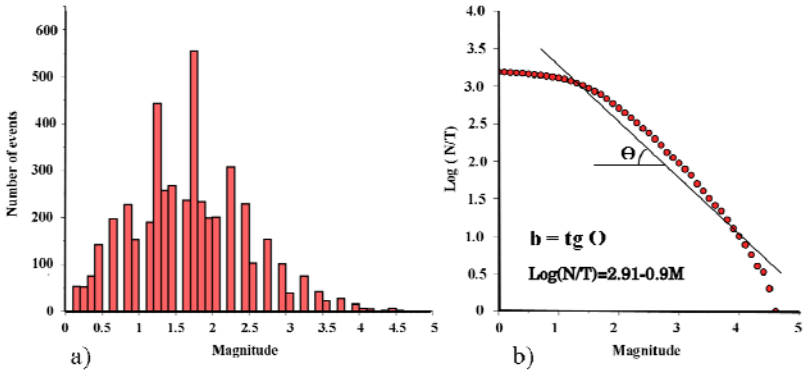

Figure10. (a) The histogram of magnitude range of 3 years micro-earthquakes recorded with the IGUT and local networks, (b) The plot of magnitude versus logarithm of the cumulative number of the earthquakes per year which gives b-value deduced by the dip of the diagram. The fitted line to linear part of the diagram was drawn using least square method.

6 Seismicity parameters

The b-value of the area could be specified using 1956 Gutenberg-Richter (G-R) formula (1). The G-R relation has often been interpreted in terms of power-law (fractal) statistics of the faults. The value of b which is the ratio of the occurrence probability of small to big earthquakes has inverse proportion to the resistance of the area against earthquake happening. This value is independent of the magnitude of the earthquakes Fig. 10a, therefore could be specified using the local events. Great b-values have been reported for background seismicity. The b-value usually is varied between 0.6 and 1.1 (Lee et al., 2002) except when a swarm of earthquakes occurs.

$$\text{Log } (N/T) = a - bM,\ N = \int_M^{\infty} N(M)dM \qquad (1)$$

In this relationship N is cumulative number of the earthquakes, T is duration of the earthquakes occurrence, M is the magnitude and a, is the seismicity trait and property of the area. According to the Fig. 10b the b-value is the tangent of the diagram dip (Θ) and equals to 0.9.

7 Conclusion

The calculated crustal velocity model is comparable with velocity model of central Alborz deduced by Ashtari et al. (2005). The sedimentary cover depth is suggested near 4 km. From the depth distribution of the earthquakes recorded by the local networks during 2007 and 2008, we estimated seismogenic zone thickness about 24 km at the east Alborz and it is the same comparing with the central Alborz deduced by Ashtari et al. (2005). Regarding to the distribution pattern of the earthquakes, the seismic activity has been concentrated around Astaneh and North Semnan faults. Both IGUT and local networks seismicity distribution patterns confirm the activity of the western segments of Shahruod fault system. Micro seismic survey confirms morphotectonic investigation, left lateral alluvial fan deposits displacement concluded reconstructing Lalun Formation, which shows Astaneh fault left lateral movement.

The Astaneh fault seismicity dips are high angle as obtained in geological investigation in surface (GSI) and confirms north partitioned segment is seismically more active. Tatar et al., 2007 mentioned that there is not flower structure in central Alborz between Khazar and Mosha faults in spite of Allen et al. (2003) idea. Map of the focal mechanisms and P and T axes shows general shortening in direction of NE-SW and extension in direction of NW-SE. Also the map shows the crust movement directions resulted from local network around the Astaneh fault and the correspondence with the GPS measured direction (Vernant et al., 2004a, b). The b-value as one of the

important seismicity parameters was obtained about 0.9 at the east Alborz. This value which is proportion inversely to the short term background seismicity intense at the east Alborz, is between of Zagros (b ~ 1) and Kopet Dagh (b ~ 0.7).

Acknowledgements

Thanks to Geological Survey of Iran for provision seismological instruments, field logistic and to the Geophysics Institute of the University of Tehran for giving data of IGUT network. Thanks especially to Professor Denis Hatzfeld (University of Joseph Fourier, France) for giving his computer programs. Thanks to Dr Ali Moradi and Dr Mohammad Tatar for scientific negotiation about the software and site selection for installing the instruments. Thanks to the people of Semnan province and especially the local governor authorities of city of Foolad-Mahalleh.

References

Abbassi, A., Nasrabadi, A., Tatar, M., Yaminifard, F., Abbassi, M., Hatzfeld, D. and Priestley, K., 2010, Crustal velocity structure in the southern edge of the Central Alborz (Iran), J. Geodyn., **49**, 68-78.

Allen, M. B., Ghassemi, M. R., Shahrabi, M., and Qorashi, M., 2003, Accommodation of late Cenozoic oblique shortening in the Alborz range, Iran, J. Struct. Geo., **25** 659-672.

Ambraseys, N. and Melville, C., 1982, A history of Persian earthquakes, Cambridge University Press, New York.

Ashtari, M., Hatzfeld, D. and Kamalian, N., 2005, Microseismicity in the region of Tehran, Tectonophysics, **395**, 193-208.

Asudeh, I., 1982, Seismic structure of Iran from surface and body wave data, Geophys. J. R. Ast. Soc., **71**, 715-730.

Berberian, M., 1983, The southern Caspian: acompressional depression floored by a trapped, modified oceanic crust, Canad. J. Earth Sci., **20**, 163-183.

Berberian, M. and King, G. C. P., 1981, Towards a paleogeography and tectonic evolution of Iran, Canadian J. Earth Sci., **18**, 210-265.

Berberian, M., Qorashi, M., Shoja-Taheri, J. and Talebian, M., 1996, Seismotectonic and earthquake-fault hazard investigations in the Semnan region. Contribution to the Seismotectonics of Iran, Part VII, Geol. Surv. Iran, **63**, 277 pp. (in Persian).

Dehghani, G. A. and Makris, J., 1984, The gravity field and crustal structure of Iran, Neues Jahrb.Geol. Palaontol. Abh., **168** 215-229.

Engdahl, E. R., Vander Hilst, R. D. and Buland, R. P., 1998, Global teleseismic earthquake relocation with improved travel time sand procedures for depth determination, Bull. Seismol. Soc. Am. **88**, 722-743.

Hollingsworth J., Jackson J., Walker R. and Nazari H., 2008, Extrusion tectonic and subduction in east South Caspian Region since 10 Ma, Geology, **36**(10), 763-766.

Jackson, J., Priestley, K., Allen, M. and Berberian, M., 2002, Active tectonic of the South Caspian Basin, Geophys. J. Int., **148**, 214-245.

Kissling, E., 1988, Geotomography with local earthquake data, Rev. Geophys., **26**, 659-698.

Lee, W. H. K. and Lahr, J. C., 1972, HYPO71(revised), A computer program for determining hypocenters, magnitude and first motion pattern of local earthquakes, U. S. Geol. Surv. Open File Rep., 75-311.

Lee, W. H., Kanamori, H., Jennings, P. C., and Kisslinger, C., 2002, International handbook of earthquake and engineering seismology, IASPEI.

Nemati, M., Hatzfeld, D., Gheitanchi, M. R., Sadidkhouy, A., Mirzaei, N., Moradi, A. S., 2010, Investigation of seismicity of the Astaneh fault in the Eastern Alborz, Journal of Earth and Space physics, Institute of Geophysics, University of Tehran, **37**(2), 1-16.

Radjaee, A. H., Rham, D., Mokhtari, M., Tatar, M., Priestley, K. and Hatzfeld, D., 2010, Variation of Moho depth in the Central part of Alborz Mountains, North of Iran, GJI, **181**, 173-184.

Ritz, J.-F., Nazari, H., Ghassemi, A., Salamati, R., Shafei, A., Solaymani, S., and Vernant, P., 2006, Active transtension inside central Alborz: A new insight into northern Iran-southern Caspian geodynamics, Geology, **34**, 477-480, doi:10.1130/G22319.1.

Samadian, M., Nabavi, M., Alavi, M., Shahrabi, M., Hamedi, A., 1975, Geological map of Semnan, scale 1:250,000, Geological Survey of Iran.

Sengo¨r, A. M. C., Altiner, D., Cin, A., Ustaomer, T., Hsu, K. J., 1988, Origin and assembly of the Tethyside orogenic collageatthe expense of Gondwana Land. Gondwana and Tethys. In: Audley-Charles, M. G., Hallam, A. (Eds.), Geological Society Special Publication **37**, 119-181.

Sodoudi, F., Yuan, X., Kind, R., Heit, B. and Sadidkhouy, A., 2009, Evidence for a missing crustal root and a thin lithosphere beneath the central Alborz by receiver function studies, Geophys. J. Int. **177**, 733-742.

Stöcklin, J., 1974, Northern Iran: Alborz mountains, in Mesozoic–Cenozoic Orogenic Belts: Datafor Orogenic Studies, ed. Spencer, A., Geol. Soc. Spec. Publ. London, **4**. 213-234.

Tatar, M., Jackson, J., Hatzfeld, D. and Bergman, E., 2007, The 2004 May 28 Baladeh earthquake (Mw 6.2) in the Alborz, Iran: over thrusting the South Caspian Basin margin, partitioning of oblique convergence and the seismic hazard of Tehran, Geophys J. Int., **170**, 249-261.

Vahdati, F. and Saidi, A., 1991, Geological map of Sari, scale 1:250,000, Geological Survey of Iran.

Vernant, Ph., Nilforoushan, F., Che´ry, J., Bayer, R., Djamour, Y., Masson, F., Nankali, H., Ritz, J.-F., Sedighi, M., and Tavakoli, F., 2004a, Deciphering oblique shortening of central Alborz in Iran using geodetic data, Earth and Planetary Science Letters, **223**, 177-185.

Vernant, P., Nilforoushan, F., Hatzfeld, D., Abassi, M., Vigny, C., Masson, F., Nankali, H., Martinod, J., Ashtiani, A., Bayer, R., Tavakoli, F., and Che'ry, J., 2004b, Contemporary crustal deformation and plate kinematics in Middle East constrained by GPS measurements in Iran and northern Oman, Geophys. J. Int. **157**, 381-398.

Wadati, A., 1933, On travel time of earthquake waves, part II., Geophys. Mag. (Tokyo), **7**, 101-111.

Appendix 1. Focal characteristics